Journal of ELECTRONIC MATERIALS, Vol. 44, No. 6, 2015
DOI: 10.1007/s11664-014-3531-5
© 2014 The Minerals, Metals & Materials Society

CrossMark

System for Simultaneous Harman-Based Measurement of All Thermoelectric Properties, from 240 to 720 K, by Use of a Novel Calibration Procedure

D. VASILEVSKIY,[1,2,4] J.-M. SIMARD,[3] R.A. MASUT,[1] and S. TURENNE[1]

1.—Département de Génie Mécanique et Département de Génie Physique, Polytechnique Montréal, C.P. 6079, Succ. Centre-Ville, Montreal, QC H3C 3A7, Canada. 2.—TEMTE Inc, 4665 West Broadway, Montreal, QC H4B 2A7, Canada. 3.—EXAPROM Inc, 40 Saint-Ange, Blainville, QC J7B 1X1, Canada. 4.—e-mail: dvasilevskiy@polymtl.ca

The most reliable evaluation of the thermoelectric (TE) figure of merit (ZT) is based on the Harman method, because the physical properties are measured on the same specimen and in the same direction. However, practical realization of this procedure at elevated temperatures is challenging, because of unavoidable heat exchange between the sample and its environment. We report the first successful implementation of this method for simultaneous measurement of the figure of merit, the Seebeck coefficient, and electrical and thermal conductivity on the same specimen in the temperature range 240–720 K, a range which covers most practical TE applications ranging from cooling to energy harvesting at both low and intermediate temperatures. The system we have developed (ZT-Scanner) automatically measures, under vacuum conditions, the properties of specimens from 1 to 6 mm long with cylindrical or rectangular ($\sim$25 mm^2) cross sections. The reproducibility of consecutive measurements was found to be 1–2% of the absolute values of the four properties, in any arbitrary temperature range. The novel two-sample system calibration (2SSC) developed resolves, irrespective of specimen size, geometry, and thermal conductivity, the unavoidable heat exchange between the specimen and the environment, assisting these measurements. We report detailed results from successful implementation of 2SSC for TE characterization of bismuth telluride-based materials from 240 to 450 K and of a large group of other materials including lead telluride, skutterudites, Mg, Si, Sn, and SiGe from 300 to 720 K. The developed ZT-Scanner in combination with the novel 2SSC procedure solve the persistent problem of accurate determination of ZT and its components and can serve as an important instrument for precise evaluation of well-established and new TE materials.

Key words: Figure of merit, thermoelectric measurements, ZT-Scanner, Harman method

INTRODUCTION

The dimensionless thermoelectric (TE) figure of merit ZT (where T is the temperature in Kelvin, and $Z = \alpha^2/\rho\lambda$ where α, ρ, and λ are, respectively, the Seebeck coefficient, the electrical resistivity, and the thermal conductivity) is the main property enabling comparison of the overall performance of different TE materials at different temperatures. Despite its extreme importance, methods of accurate measurement of its value are very limited. Currently, the most widely used approach separately measures each of the components of ZT. The main problem

(Received June 10, 2014; accepted November 11, 2014; published online December 4, 2014)

with this approach is that it requires at least two different samples, one to determine α and ρ and a second for measurement of λ. The Seebeck coefficient/electric resistance measurement system (ZEM) from Ulvac is frequently used to determine both α and ρ, leading to uncertainties of approximately 5% for α and 10% for ρ, as reported by Wang et al.[1] Thermal conductivity can be measured by use of different methods;[2,3] the laser flash technique[3] implemented by use of the Netzsch LFA 457 combined with a differential scanning calorimeter (Netzsch DSC 204) for measurement of specific heat is the most common.

This approach led to total uncertainty in *ZT* evaluated in Wang et al.[3] and by Snyder and Toberer[4] as high as 40–50%, which is unacceptable in most scientific and industrial applications. Sometimes,[5,6] separate measurements can be made on the same sample and in the same direction during one measurement cycle, which reduces uncertainty to approximately 25% (ZT-Meter-870 K; developed by the Fraunhofer Institute for Physical Measurement Techniques, Germany), which is still too high. This uncertainty leads to critical overestimation or underestimation of the actual performance of a TE material and in some cases may lead to misleading research conclusions.

The most accurate *ZT* value can potentially be obtained by use of the Harman method[7,8] and its modification,[9] which are used for direct evaluation of the TE figure of merit on a single specimen. We will discuss the advantages of this method later. However, from the very first publications[7–9] up to the most recent[10–12] the effect of parasitic heat exchange between the sample and its environment has been identified as critical for measurement accuracy. This effect was studied theoretically for specific conditions[2,10] and has been evaluated by fitting data for a variety of sample geometries and specific contact wire diameters.[11] It was found that the effect of these parasitic thermal phenomena usually increases rapidly with measurement temperature, necessitating use of correction coefficients up to 80% of the measured *ZT* value, which could not be reliably evaluated for arbitrary temperatures and sample size. This fact has seriously reduced application of Harman based measurements, especially at elevated temperatures, at which radiation losses increase rapidly.

We describe here a novel calibration procedure which is intended to radically solve the problem of parasitic thermal phenomena. Novel two-sample system calibration (2SSC) has been successfully implemented by use of a system (ZT-Scanner; Temte) developed for simultaneous Harman based measurement of all TE data from 240 to 720 K. We report how the developed system works with different materials and sample size. We have limited this discussion to measurements above room temperature because this temperature range is the most critical.

BASIC PRINCIPLES AND SYSTEM CONFIGURATION

The ZT-Scanner implements the Harman method on the basis of the sample configuration shown schematically in the inset of Fig. 1.

Physically the ZT-Scanner consists of two rack mounted blocks:

1. A functional block which includes the pumping unit and a vacuum chamber with the sample holder (photograph in Fig. 1) that can be cooled or heated and provides constant temperature throughout the measurement; and
2. A computer-controlled data-acquisition unit, which includes a Keithley 2401 high-precision programmable direct-current (DC) power source, an Agilent 34420a nano-voltmeter, and an Agilent 34970a switch unit.

We use samples with a rectangular cross section, $5 \times 5 \times 6$ mm^3, as standards; however other sample sizes and geometry can also be used. We will discuss later how to ensure correct measurements for samples different sizes. We use a "two-point" sample setup option, as described in Wang et al.[1] We supply four wires and two thermocouples, but the common points for electrical current and voltage wires at both extremities of the sample are on the copper contact plates (inset in Fig. 1). The bottom of the sample is placed on top of a copper sample holder and is covered by an aluminum thermal shield, as shown in Fig. 1. The temperature of the sample can be varied from 300 to 720 K by computer-controlled heating and stabilization of the high temperature sample holder.

Measurement of TE properties by use of the ZT-Scanner is based on implementation of a bipolar Harman procedure[9] (Fig. 2) in which a direct electrical current I_{DC} circulates through the sample for a period of time deemed sufficient for stabilization of

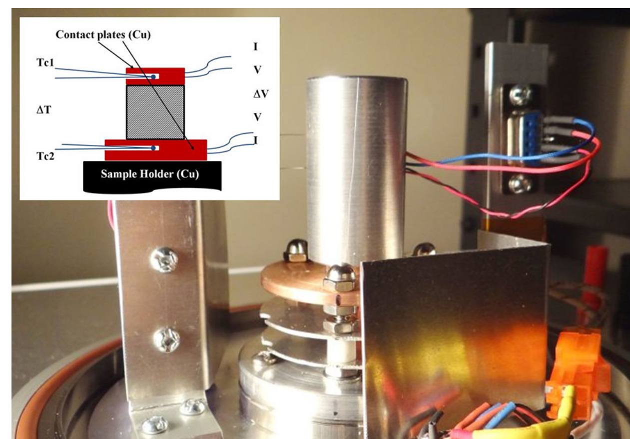

Fig. 1. Image of the vacuum chamber with the high temperature sample holder (Cu block) covered by an cylindrical aluminum thermal shield. The inset shows a schematic representation of the sample-measurement setup.

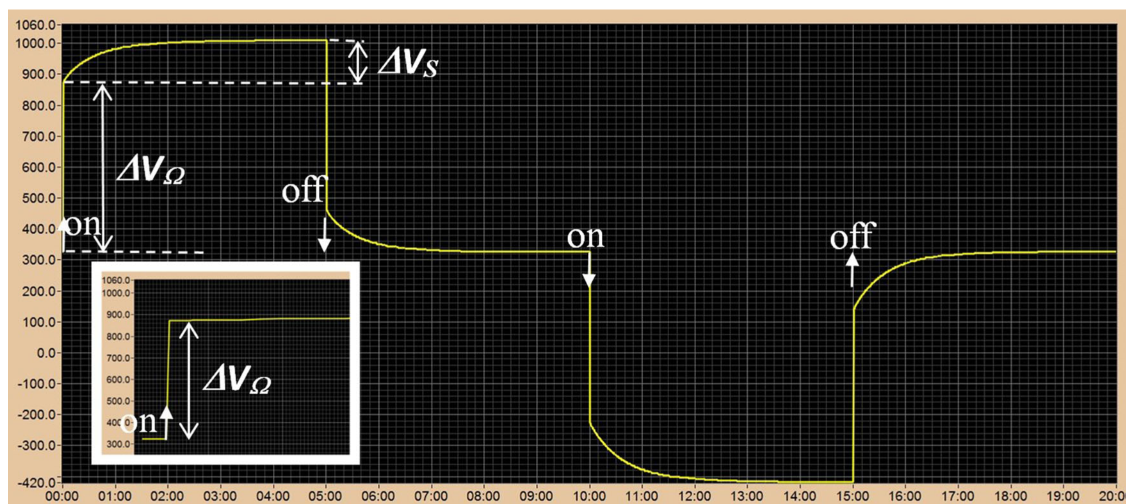

Fig. 2. A computer screen shot of the voltage across the sample during the 20-min Harman test, with the inset showing an enlarged horizontal scale during the first 10 s. Current "on" and current "off" points with reversed polarities are identified by arrows.

the conditions. The voltage and temperature are simultaneously measured on both extremities of the sample to determine the corresponding values of ΔV and ΔT. The electrical resistivity of the sample is given by $\rho = SF \times \Delta V_{\Omega}/I_{DC}$, where $SF = A/l$ is the sample shape factor, or geometric aspect ratio, for a sample cross-sectional area A and sample thickness l. The Seebeck coefficient can be obtained from $\alpha = \Delta V_S/\Delta T$. The dimensionless TE figure of merit, for currents low enough to enable Joule heating effects to be neglected, is $ZT = T(\Delta V_S/\Delta V_{\Omega})$. The thermal conductivity is $\lambda = \alpha^2/Z\rho$. The Harman-based test enables the four TE variables to be obtained for the same sample during one measurement cycle. The accuracy of the method requires that measurement be performed under adiabatic condition (absence of loss or gain of heat). However, this condition is never achieved in practice for any Harman setup. We will discuss below how to avoid important offsets in results originating from parasitic heat exchange between the sample and its environment.

During a Harman test the temperature of the sample holder remains steady at the given measurement point. Figure 2 shows a typical pattern of the Harman test as a computer screen shot. In the figure we see the voltage drop (scale in μV) between the two sample extremities as a function of time (min). The test was performed on a PbTe sample at 395 K using a DC of 100 mA. Using two "current-ON" and two "current-OFF" switches to reverse the polarity we collect four values of each TE variable, and generate average values for ρ, ZT, α, and λ for the given temperature.

RESISTIVITY AND SEEBECK COEFFICIENT MEASUREMENTS

Use of a two-point resistivity measurement setup, shown schematically in the inset of Fig. 1, means that the electrical resistance of the interface's sample-contact plate should be negligible. Samples soldered with PbSn or SnSb alloys as contact materials ensure accurate measurement up to 450 K. For measurements up to 720 K contacts may be easily obtained by use of silver paste. In all cases we recommend previous electro or vacuum plating of the two sample contact surfaces with Ni (2–3 μm), to prevent inward diffusion of the contact material. The criteria for accuracy of the resistivity measurement are the comparative values of the sample and the contact resistances. Direct measurement of the specific contact resistivity, conducted when the two contact plates are inter-soldered with the same alloy as used for the sample contacts, gives a value $6 \pm 0.6 \times 10^{-7}\ \Omega\ \mathrm{cm}^2$. For silver paste using the same method we found three different room temperatures of the contact resistance (R_{cont}). After curing for 1 h in air at 200°C, in accordance with the instructions of the paste manufacturer, the specific contact resistivity reaches a value equal to or larger than $7 \times 10^{-6}\ \Omega\ \mathrm{cm}^2$. However, we observed a gradual decrease of R_{cont} during consecutive heat treatment: first up to 570 K and second up to 730 K, both under vacuum. The room temperature contact resistivity decreases to $2.5 \times 10^{-6}\ \Omega\ \mathrm{cm}^2$ and $9 \times 10^{-7}\ \Omega\ \mathrm{cm}^2$, respectively. We also measured the contact resistance of the silver paste at high temperatures when the copper blocks were electroplated with Ni, as for the TE alloy samples, and obtained values as low as $5 \times 10^{-6}\ \Omega\ \mathrm{cm}^2$ at 726 K.

In Table I we show the effect of finite values of the contact resistance Rcont (evaluated as indicated in the previous paragraph) on the accuracy of the resistivity for a TE material of nominal size $5 \times 5 \times 6\ \mathrm{mm}^3$, for different contact options and for four hypothetical values of the sample resistivity ρ. Choice of a nominal sample size of $5 \times 5 \times 6\ \mathrm{mm}^3$ to calculate, from Rcont, the equivalent additional resistivity, may seem arbitrary but it was chosen

Table I. Effect of different contact options on measured values of electrical room temperature-specific contact resistivity

Contact option	PbSn soldered	1 h curing, 200°C, air	Additional 570 K curing, under vacuum	Additional 730 K curing, under vacuum
300 K specific contact resistivity (Ω cm^2)	6×10^{-7}	$\geq 7 \times 10^{-6}$	2.5×10^{-6}	9×10^{-7}
Equivalent resistivity (ER) ($\mu\Omega$ m)	1.3×10^{-2}	$\geq 15 \times 10^{-2}$	5×10^{-2}	2×10^{-2}
ER relative to 2 $\mu\Omega$ m	0.65%	≥7.5%	2.5%	1%
ER relative to 5 $\mu\Omega$ m	0.26%	≥3.0%	1.0%	0.4%
ER relative to 10 $\mu\Omega$ m	0.13%	≥1.5%	0.5%	0.2%
ER relative to 20 $\mu\Omega$ m	0.065%	0.75%	0.25%	0.1%

The last three columns apply to silver paste contacts.

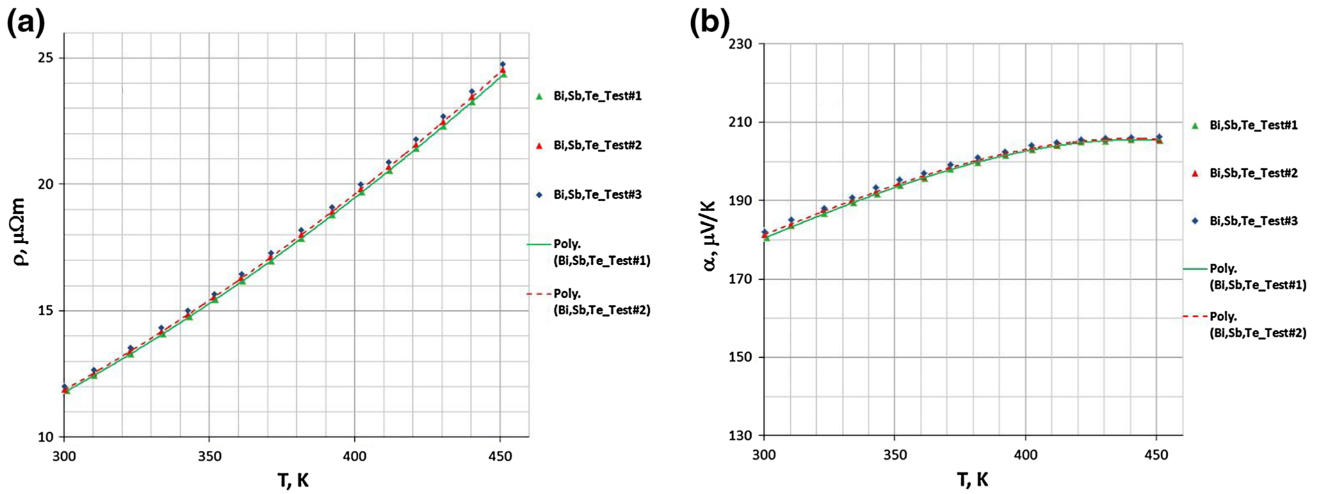

Fig. 3. Measurement of electrical resistivity (a) and Seebeck coefficient (b) in three consecutive temperature runs on one sample of hot extruded *p*-type bismuth telluride-based material.

because it is the value recommended for the ZT-scanner.

Table I shows that overestimation of the electrical resistivity for most realistic examples ($\rho \geq 5$ $\mu\Omega$ m) is $<1\%$. Silver paste cured for 1 h at 200°C in air is the only contact that would not be recommended for measurement of a highly conductive material. All four values of the electrical resistivity of the hypothetical TE material quoted in Table I completely cover the range of values of ρ for state-of-the-art TE materials.

For new materials under development, for which the electrical resistivity is usually much higher that the values considered in Table I, the effect of the contact resistance is negligible.

Another source of error in resistivity measurement is uncertainty in the evaluation of sample size. For the ZT-Scanner the distance between the contacts can be easily measured with precision of 0.01 mm, because the contacts are applied directly to the sample surface. The combined uncertainty for the square section and length measurement is of the order of 0.6%. This is a huge advantage compared with other apparatus using four-point setup, for example the ZEM-3, for which this error leads to uncertainty in ρ values of up to 10%.[1] Because the error of the Keithley 2401 power source and of the Agilent 34420a nano-voltmeter are $<0.1\%$ we assume the total measurement error of the electrical resistance is usually less than 1%. Note that the contact options described are those which we found easy to use and reliable; other options which ensure low contact resistivity[13] can be equally used for sample mounting on the ZT-Scanner.

The Seebeck coefficient is evaluated directly as the ratio $\alpha = \Delta V_S / \Delta T$ of the Seebeck voltage drop and the temperature drop produced during the Harman test across the sample by Peltier heating. The inset of Fig. 2 shows that the two components ΔV_Ω and ΔV_S of the total voltage drop can automatically be easily separated by the different relaxation times of electronic and thermal phenomena with accuracy of 1% by use of the appropriate algorithm and by avoiding user effects.

The total relative error for either temperature or voltage measurements is about 0.2% for the data acquisition unit of the ZT-Scanner.

Figure 3 shows results obtained from measurement of electrical resistivity and Seebeck coefficient in three consecutive temperature runs on one sample

Table II. ZT and λ values obtained for two samples of different length, l, by use of the same correction polynomial

	300 K		450 K		600 K	
Sample l (mm)	8.31	3.49	8.31	3.49	8.31	3.49
ZT	0.239	0.245	0.432	0.451	0.445	0.571
λ (W/m K)	2.83	2.74	2.14	1.93	2.09	1.59

of hot extruded p-type bismuth telluride-based material. A PbSn soldered alloy was used as the contact over electroplated Ni.

The third-order polynomial trend lines shown in Fig. 3 for the first and the second tests are within 1% of the respective absolute values, confirming the high reproducibility and precision of the ZT-Scanner system.

ZT AND Λ MEASUREMENTS: TWO-SAMPLE SYSTEM CALIBRATION (2SSC) PROCEDURE

For Harman-based measurement of the TE figure of merit, defined as $ZT = T(\Delta V_S/\Delta V_\Omega)$, assuming adiabatic conditions, as discussed above, we emphasize that the measured ZT value is not obtained from separately measured ρ, α, and λ, but is the result of direct measurement of two voltage drops ΔV_S and ΔV_Ω. Not even sample size is involved in its calculation and has no effect on its accuracy. The temperature and the voltage values can be measured with an error not exceeding 0.2% if a high quality nano-voltmeter is used. The two parts of the voltage drops could be easily separated, as shown in the inset in Fig. 2.

However, as we discussed in the "Introduction", the real problem associated with this approach originates from the difficulty of estimating the effect on the measurement of heat exchange between the sample and its environment, which compromises the adiabatic conditions. Simultaneous action of several phenomena, for example the thermal conductance of the wires and the thermocouples, radiation losses, and thermal conductance and convection of the residual atmosphere have been studied[10] and theoretical predictions were found not realistic for practical use. The adiabatic conditions will be further compromised when the temperature of the test is increased. This issue can be solved for well-known materials if a reference sample can be used for calibration of the ZT value, but this approach fails if samples of different size are measured. Table II illustrates the difference between the ZT and λ values obtained for two samples of the same cross-section and different lengths cut from the same homogeneous extruded PbTe rod. For both samples the same correction polynomial obtained by use of a reference sample was used.

The reason for the observed differences is the effect of the parasitic thermal conductance from the sample to its environment. In our case the "short" sample has a 2.38 times higher thermal conductance than the "long" one and, in fact, needs a lower correction coefficient for ZT and λ values. Similarly, for the "long" sample with a lower intrinsic conductance, the effect of the thermal losses is proportionally larger, and a higher correction factor should be applied. This situation becomes even more complex if not only the geometrical aspect ratio varies from sample to sample but also the thermal conductivity of the material to be measured.

To solve this problem, which requires individual correction for each sample to obtain an accurate measurement result, we have developed a novel system calibration procedure which we call 2SSC. Keeping in mind that precise theoretical prediction of all thermal interactions of the sample with its environment is unrealistic, we succeeded instead in experimentally defining the total effect of all parasitic phenomena at any given temperature. We now describe this procedure, as a sequence of two steps.

First Step of the 2SSC Procedure

The theoretical background for the first step of the 2SSC procedure relies on the simple statement that Peltier heat αTI during the Harman test, at fixed temperature T and electric current I, generates a temperature difference ΔT_S across the sample which is inversely proportional to the thermal conductance of the sample K_s and the total equivalent thermal conductance K_p of all parasitic radiation and thermal conductance phenomena. The thermal conductance K_p is considered here to be independent of sample geometrical aspect ratio SF, when the sample height is from 2 to 7 mm, the limits recommended for the ZT-Scanner. Note that this statement is at this point only hypothetical and must be validated, as we will show in the section "Experimental Validation of 2SSC Procedure".

Application of this statement on the temperature difference generated by the Peltier effect for two samples of the same material and different aspect ratios results on the following system of two equations:

$$\begin{cases} \alpha TI = \Delta T_1(K_{s1} + K_p) \\ \alpha TI = \Delta T_2(K_{s2} + K_p) \end{cases}. \quad (1)$$

Notice that the Joule heat exchange of the upper side wire has not been included in the thermal

balance. This is correct because we have already averaged the ΔT_s values for both polarities of the DC current (Fig. 2), which excludes its effect.[9] Also, there is no effect of the bottom side wire by default, because the temperature of the sample at this point corresponds to the temperature of the sample holder and remains constant during the Harman test.

When the lengths of the two samples are related by $l_1 = nl_2$, and the square sections of the samples are the same, the shape factors of the first and the second samples are related by the expression $nSF_1 = SF_2$. For both samples which are cut from the same material with the same thermal conductivity, we can write $K_{s1} = nK_{s2}$. Introducing this in the second equation of Eq. 1 we can solve for the parasitic conductance:

$$K_p = K_{s1}\frac{n\Delta T_2 - \Delta T_1}{\Delta T_1 - \Delta T_2}. \quad (2)$$

The value of the TE figure of merit can be expressed on the basis of the internal material properties α, λ, and ρ or on the basis of the electric resistance, R_{s1}, and thermal conductance, K_{S1}, of the first sample:

$$ZT = \frac{\alpha^2}{\rho\lambda} = \frac{\alpha^2}{R_{s1}K_{s1}}. \quad (3)$$

Measurement of the first sample, which in practice cannot avoid thermal losses, without any calibration, defines the value $Z_{1meas}T$ and λ_{1meas}

$$Z_{1meas}T = \frac{\alpha^2}{R_{s1}(K_{s1}+K_p)} = \frac{\alpha^2}{R_{s1}K_{s1}\left(1+\frac{K_p}{K_{s1}}\right)}. \quad (4)$$

Combining Eqs. 2, 3, and 4 we can find the relationship between the proper ZT and λ values of the material and the raw data of the Harman measurement on the first sample:

$$ZT = Z_{1meas}T\left(1+\frac{n\Delta T_2 - \Delta T_1}{\Delta T_1 - \Delta T_2}\right) \quad (5)$$

$$\lambda = \lambda_{1meas}/\left(1+\frac{n\Delta T_2 - \Delta T_1}{\Delta T_1 - \Delta T_2}\right). \quad (6)$$

Remembering that $K_{s1} = nK_{s2}$ we can also express the real values of the material properties by using the raw data collected for the second sample:

$$ZT = Z_{2meas}T\left(1+\frac{1}{n}\frac{K_p}{K_{s1}}\right) = Z_{2meas}T\left(1+\frac{1}{n}\frac{n\Delta T_2 - \Delta T_1}{\Delta T_1 - \Delta T_2}\right) \quad (7)$$

$$\lambda = \lambda_{2meas}\Big/\left(1+\frac{1}{n}\frac{K_p}{K_{s1}}\right) = \lambda_{2meas}\Big/\left(1+\frac{1}{n}\frac{n\Delta T_2 - \Delta T_1}{\Delta T_1 - \Delta T_2}\right). \quad (8)$$

Equations 5, 6, 7, and 8 show that the true ZT and λ values can be assessed equally for both samples, however the shorter sample needs smaller correction. Note, that for this correction factor we are not using any of the material properties, only values of measured temperature drops generated by Peltier heating of the first and second samples when the same current is used.

Second Step of the 2SSC Procedure

We have demonstrated how the true ZT and λ values can be defined by using two samples of different lengths cut from the same material. However, this procedure is time consuming and may not always be applicable. For example it might be impossible to prepare two differently sized samples with exactly the same internal properties. If, on the other hand, the described procedure were to be performed on the measurement system at least once, it will provide a correction of the ZT and λ values, and also the absolute parasitic thermal conductance by use of Eqs. 2 and 6 and the SF_1 value for the first sample.

As we saw in the previous section, this parasitic conductance becomes the distinctive system parameter, which varies with temperature but for all practical purposes is independent of sample size and nature. This is essentially because its inherent losses have been minimized and are negligible in comparison with those of the measurement system, which are taken into account by the calibration procedure.

Considering the first sample as the reference sample we can calculate the ratio of the two thermal conductances K_p/K_{ref}. This means that if the second sample is the unknown one which we want to characterize (referred to as the sample x), we can write equations similar to Eqs. 7 and 8:

$$Z_X T = Z_{X,meas}T\left(1+\frac{1}{n}\frac{\lambda_{Ref}}{\lambda_X}\frac{K_p}{K_{Ref}}\right) \quad (9)$$

$$\lambda_X = \lambda_{X,meas}\Big/\left(1+\frac{1}{n}\frac{\lambda_{Ref}}{\lambda_X}\frac{K_p}{K_{Ref}}\right). \quad (10)$$

In Eqs. 9 and 10 the new term λ_{Ref}/λ_X has appeared because sample x differs from the reference one not only in shape but also in thermal conductivity with $K_X = n\frac{\lambda_X}{\lambda_{Ref}}K_{Ref}$. Equation 10 can be solved for λ_X:

$$\lambda_X = \lambda_{X,\mathrm{meas}} - \frac{\lambda_{\mathrm{Ref}}}{n}\frac{K_p}{K_{\mathrm{Ref}}}. \quad (11)$$

Using this value in Eq. 9 we obtain the real figure of merit $Z_X T$ for the unknown sample x, which is the objective of the measurement.

EXPERIMENTAL VALIDATION OF 2SSC PROCEDURE

For practical realization of this calibration procedure two directly adjacent samples (inset in Fig. 4) were cut from a PbTe hot extruded rod. The high homogeneity of the extruded TE material[14–16] ensures that the thermal conductivity and other properties of both samples are the same. The dashed lines in Fig. 4 show the raw results from the measurements without any calibration. As is to be expected, the shorter sample has a higher $Z_{\mathrm{meas}}T$ value and a lower λ_{meas} value than the longer sample.

The ZT-Scanner not only provides the time-resolved value of the voltage drop for the sample but also temperature variations on both its contact sides, which enables precise measurement of the ΔT_1 and ΔT_2 values which are used for the 2SSC. Continuous lines correspond to the trend lines of the ZT and λ values for both long and short samples after correction by the first step of the 2SSC procedure, as described above. It is now hard even to detect any difference between corrected values throughout the range from 300 K to 700 K. For the correction process we have used Eqs. 5 and 6 which were derived from Eq. 1. The measured quantities which we used to define the correction coefficients are the temperature differences and the ratio of sample lengths. Nowhere do we impose equal ZT and λ values for both samples, yet the results are in agreement for all temperatures after correction has been performed. We would never observe this coincidence in both sets of curves in Fig. 4 when correcting by use of Eqs. 5 and 6 if the real thermal balance differed from that described by Eq. 1. The coincidence is not automatic but actually predicted by the model, because it reflects adequate physics. In this the way we validate our hypothesis that, in our experimental set-up, the parasitic heat transfer is independent of the sample geometrical aspect ratio SF, at least for the samples used in the test with lengths between 3.96 and 6.98 mm.

Figure 5 shows that parasitic heat conductance K_P from the sample to its environment varies with temperature in close agreement with a power law with an exponent of 3.3 (continuous tendency line in Fig. 5) indicating that the main mechanism of heat loss is radiation. However, in our case the parasitic heat flow is the radiative heat exchange between the upper sample contact plate and aluminum thermal shield (Fig. 1). The shield temperature also varies with sample holder heating, which results in a deviation from the pure power law with order 4. Heat conductance K_S through the long and the short samples is also shown in the same figure. At 300 K the parasitic thermal conductance is approximately a factor of 50 lower than the heat conductance within the samples and, to a first approximation, could be neglected. However, at the elevated temperatures the situation changes drastically, as is shown in the figure. All three heat conductances become comparable near 700 K and the correction of the measured ZT and λ values is absolutely necessary. Note also that the K_P curve in Fig. 5 is the distinctive profile of the sample setup in our ZT-Scanner, and can be used for measurement and calibration with this apparatus only.

When the 2SSC procedure is performed we estimate the error of ZT and λ values to be no larger

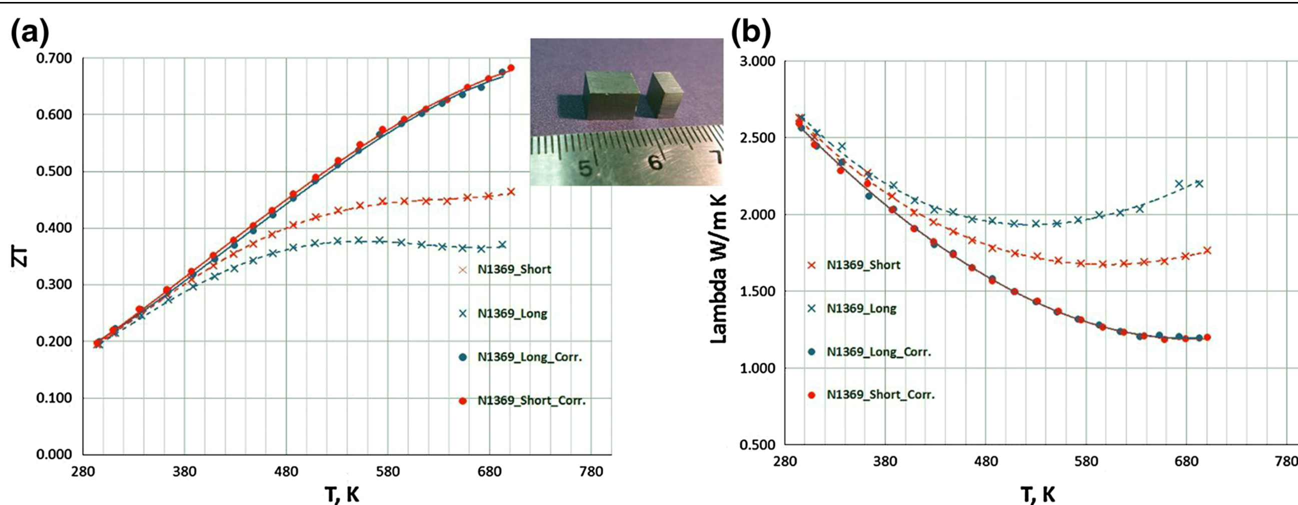

Fig. 4. ZT (a) and λ (b) values measured for two PbTe samples of identical section (27.76 mm^2) and different lengths (6.98 and 3.96 mm), before calibration (crosses joined by dashed lines), and corrected after implementing 2SSC procedure (solid circles joined by continuous lines). The two samples used for the calibration are shown in the inset (ruler scale in mm).

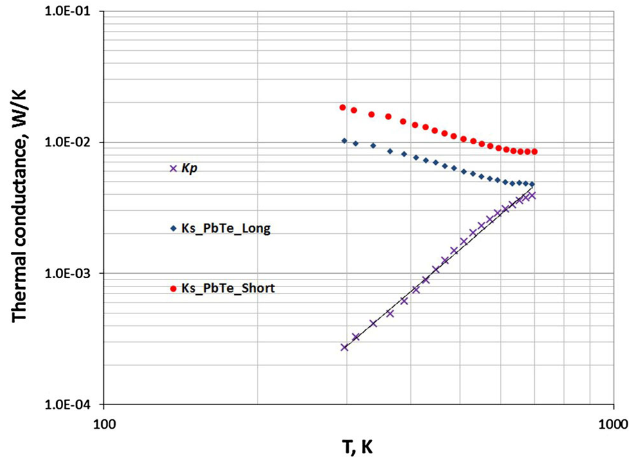

Fig. 5. Temperature dependence of the parasitic heat conductance K_P (crosses) compared with the heat conductance K_S through the long (blue diamonds) and the short (red circles) samples (Color figure online).

than 1%, because the error of the temperature difference ΔT_S generated by Peltier effect during the test and measured on the first, second, and xth sample is $< 0.2\%$ in the whole temperature range. We only perform arithmetic operations with these ΔT_S values, as follows from Eqs. 2, 9, 10 and 11, and the error propagation is limited and well known.

We only estimate here the accuracy of the measurements. Its proper evaluation will be possible only when high-temperature standard samples become available.

RESULTS OF THE APPLICATION OF THE ZT-SCANNER WITH THE 2SSC ON DIFFERENT TE MATERIALS

To demonstrate the reproducibility and versatility of the ZT-Scanner with the 2SSC data treatment incorporated in the operating software we report characterization of a variety of TE materials at temperatures in the range from room temperature to 720 K. Figure 6 shows the temperature variation of the main TE properties of hot extruded p-type BiSbTe-based and p-type SiGe-based alloys (provided by JPL), n-type skutterudite (provided by Evident Technologies), and n-type PbTe (hot extruded at Ecole Polytechnique of Montreal). The dashed line on the ZT figure shows JPL data supplied with the SiGe alloy. The results for the BiSbTe based sample, presented in Fig. 6, were assessed with PbSn soldered contacts and show three consecutive runs without opening the vacuum chamber and without any intentional changes applied to the contacts. For the other materials silver paste cured in air at 200°C followed by a vacuum curing at 550 K was used as the contact material. The measurements on the SiGe sample were repeated (Test#2) after completely removal of the contacts then electroplating with Ni and re-application of silver paste. Test#3 on the SiGe sample was performed with the same contacts without opening of the vacuum chamber between tests #2 and #3.

Materials other than those presented in Fig. 6, for example samples of MgSiSn and FeS_2 have also been successfully measured by use of our system. The samples were of different size, with the geometrical aspect ratio SF varying from 0.14 mm to 0.454 mm. Excellent reproducibility of the results, irrespective of the contact options, confirms the high reliability of the ZT-Scanner. We estimated in previous sections the accuracy for ZT and its components at the level of 1%; however, Fig. 6 shows a spread of experimental points for α measurements close to room temperature of approximately 2.2% leading to larger point dispersion for the λ values. We attribute this to the effect on these measurements of incompletely filtered electromagnetic (EM) noise, because the respective trend lines remain close to each other, mostly within 1% of the measured values.

DISCUSSION AND CONCLUSIONS

All measurement systems must comply with two main criteria: reproducibility of the results and accuracy of the absolute values. We ensured the reproducibility of consecutive measurements by working on two different levels. First, we built a data-acquisition unit containing a high-precision low-noise DC current source, a nano voltmeter, and a switch unit using appropriate wire shielding and digital signal filtering. These measures ensure reproducibility of results at the base level. As the second level we standardized the sequence of operations for sample mounting, including electroplating of an Ni layer (2–3 μm), then soldering samples to copper contact plates with PbSn alloy or using silver conductive adhesive paste followed by air and vacuum curing procedures, as already described. Thermally conducting paste was used for thermocouple mounting. Figures 3 and 6 show the excellent reproducibility of ZT, ρ, α, and λ values measured on the p-type bismuth telluride-based material and SiGe samples.

To comply with the second criterion related to the consistency of the absolute values we estimated the effect of the contact resistance and found it negligible compared with the measured material resistance, as is apparent from the values in Table I. Low specific contact resistivity and appropriate thermocouple mounting in our setup ensures accurate measurement of ρ and α. As already discussed, the accuracy of ZT and λ measurements cannot be assessed directly because of the unavoidable heat exchange between the sample and its environment compromising the adiabatic condition. Our approach accepts that precise theoretical prediction of this complex thermal interaction is unrealistic and experimentally evaluates the total effect of all parasitic phenomena for any given temperature. To avoid applying an empirical approach to each

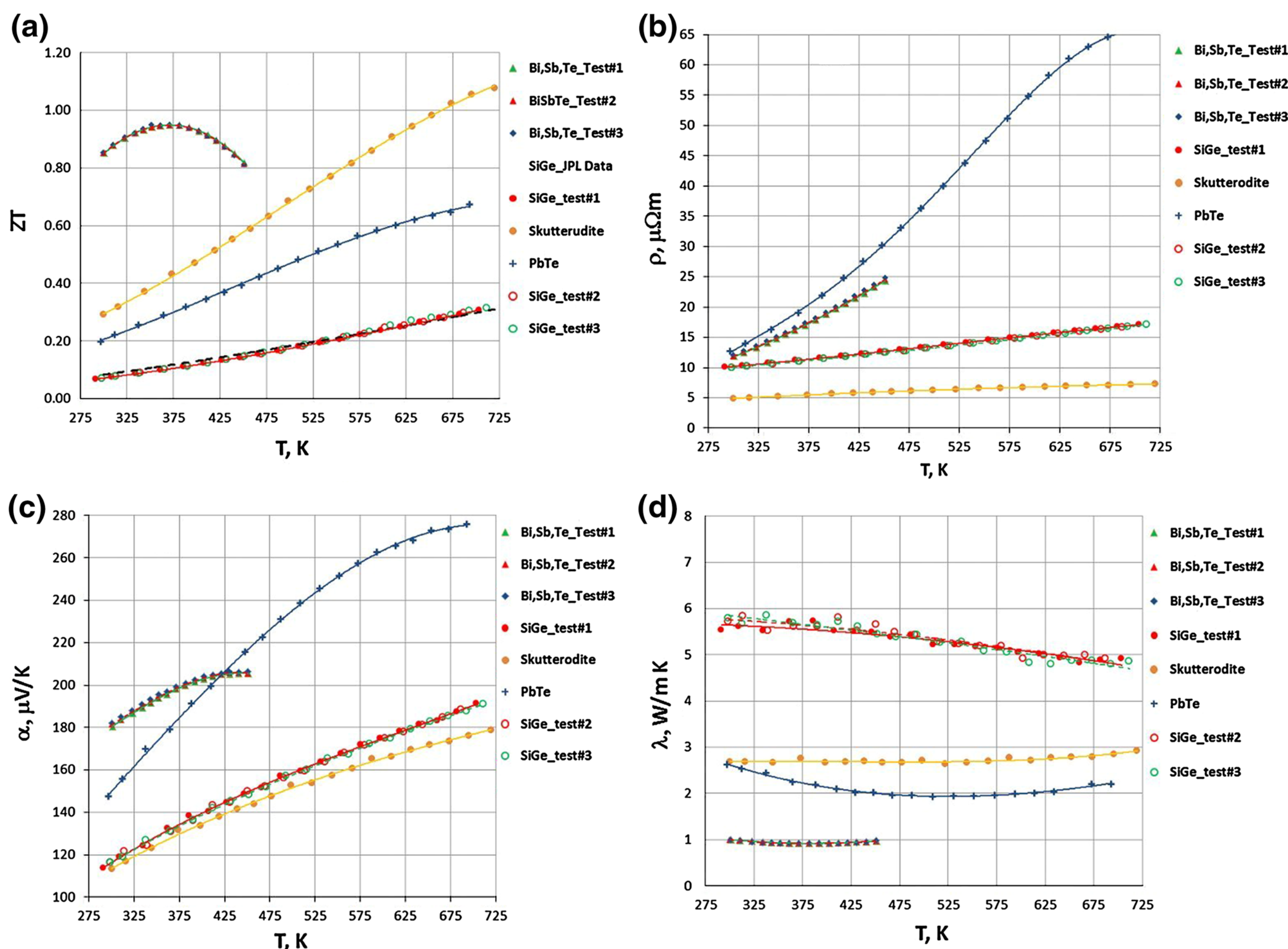

Fig. 6. Variation with temperature of *ZT* (a), ρ (b), α (c), and λ (d), measured for a set of four different TE materials with 2SSC performed on the PbTe samples of Fig. 4.The absolute values of the Seebeck coefficient were used for the *n*-type materials for presentation on a single figure with *p*-type samples.

individual sample we have developed a novel 2SSC procedure. We report detailed results from successful implementation of the 2SSC for TE characterization of bismuth telluride-based materials from 240 to 450 K and of samples from a diverse group of materials including lead telluride, skutterudites, $MgSi_2$, FeS_2, and SiGe, from 300 to 720 K. Of particular interest are the *ZT* data presented in Fig. 6, in which all the curves appear exactly as we are used to seeing them in reviews on thermoelectricity.[4] The agreement of the results obtained by use of the ZT-Scanner for the SiGe sample supplied by JPL with their reference data (Fig. 6) serves as additional confirmation of the high accuracy of the developed system and the 2SSC processing. Note that while the basic principle of 2SSC is universal, the specific values of the parasitic heat conductance at each temperature depend on the system design. This means that the results from Fig. 5 can only be used for sample setup of the ZT-Scanner (Temte) and its direct application for different designs leads to incorrect calibration. We discussed here only measurements above 300 K, because they are usually more questionable. For measurements below room temperature the ZT-Scanner is equipped with a different sample holder with a cooling module. Obviously, it requires its proper 2SSC procedure resulting in a new correction coefficient for each temperature. Because the combined parasitic thermal interactions of the sample and its environment can be evaluated experimentally with high precision (≤1%) this is no longer a critical factor and its effect on measurements can be easily compensated by proper system calibration.

We want to repeat here that the results for different materials were collected during one temperature scan on one sample for each material only a few millimeters in size. This consideration is important for new materials development, when it is frequently impossible to prepare a single specimen large enough to cut separate samples for ρ and α measurements and then for laser flash λ measurements.

The developed ZT-Scanner in combination with the novel 2SSC procedure presented in this paper solve the persistent problem of accurate and precise

determination of ZT and its components and could serve as a crucial instrument for laboratory evaluation of well-established and new TE materials.

ACKNOWLEDGEMENTS

We acknowledge financial support from the Natural Sciences and Engineering Research Council of Canada (NSERC), under the strategic project program, and of the Fonds de Recherche du Québec—Nature et Technologies (FRQNT), Projet de recherche orientée en partenariat.

REFERENCES

1. H. Wang, W.D. Porter, H. Botner, J. Konig, et al., *J. Electr. Mater.* 42, 654 (2013).
2. G.S. Nolas, J. Sharp, and H.J. Goldsmid, *Thermoelectrics; Basic Principles and New Materials Developments* (Berlin: Springer, 2001), p. 95.
3. H. Wang, W.D. Porter, H. Botner, J. Konig, et al., *J. Electr. Mater.* 42, 1073 (2013).
4. G.J. Snyder and E.S. Toberer, *Nat. Mater.* 7, 105 (2008).
5. V.K. Zaitsev, M.I. Fedorov, E.A. Gurieva, I.S. Eremin, et al., *Phys. Rev. B* 74, 045207 (2006).
6. Fraunhofer Institute For Measurements Web Site: http://www.ipm.fraunhofer.de/content/dam/ipm/en/PDFs/Product%20sheet/ES/ZT-Meter870K_web.pdf, Accessed June 07, 2014.
7. T.C. Harman, *J. Appl. Phys.* 29, 1373 (1958).
8. T.C. Harman, J.H. Cahn, and M.J. Logan, *J. Appl. Phys.* 29, 1351 (1959).
9. R.J. Buist, *CRC Handbook of Thermoelectrics* (Boca Raton, FL: CRC Press, 1995).
10. A. Jacquot, M. Jagl, J. Konig, D.G. Ebling, and H. Bottner, *5th European conference on Thermoelectrics*, (Odessa, Ukraine, 2007), pp. 90–93.
11. B. Kwon, S.-H. Baek, S.K. Kim, and J.-S. Kim, *Rev. Sci. Instum.* 85, 045108 (2014).
12. H. Iwasaki, T. Yamamoto, H. Kim, and G. Nakamoto, *J. Electr. Mater.* 42, 1840 (2013).
13. R.P. Gupta, R. McCarty, and J. Sharp, *J. Electr. Mater.* 43, 1608 (2014).
14. J.-M. Simard, D. Vasilevskiy, F. Bélanger, J. L'Ecuyer, and S. Turenne, *Proceedings 20th International Conference on Thermoelectrics*, (Beijing, China, June 2001), pp. 132–135.
15. D. Vasilevskiy, J.-M. Simard, F. Bélanger, F. Bernier, S. Turenne, and J. L'Ecuyer, *Proceedings 21st International Conference on Thermoelectrics*, (Long Beach, California, August 2002), pp. 24–27.
16. D. Vasilevskiy, R.A. Masut, and S. Turenne, *J. Electr. Mater.* 41, 1057 (2012).